Defining the structural requirements for ribose 5-phosphate-binding and intersubunit cross-talk of the malarial pyridoxal 5-phosphate synthase

Bianca Derrer [a], Volker Windeisen [b], Gabriela Guédez Rodríguez [b], Joerg Seidler [c], Martin Gengenbacher [a,1], Wolf D. Lehmann [c], Karsten Rippe [d], Irmgard Sinning [b], Ivo Tews [b,*], Barbara Kappes [a,**]

[a] University Hospital Heidelberg, Department of Infectious Diseases, Parasitology, Im Neuenheimer Feld 324, 69120 Heidelberg, Germany
[b] Heidelberg University Biochemistry Center (BZH), Im Neuenheimer Feld 328, 69120 Heidelberg, Germany
[c] German Cancer Research Center, Molecular Structure Analysis, Heidelberg, Germany
[d] German Cancer Research Center and Bioquant, Research Group Genome Organization and Function, Im Neuenheimer Feld 280, 69120 Heidelberg, Germany

ARTICLE INFO

ABSTRACT

Most organisms synthesise the B$_6$ vitamer pyridoxal 5-phosphate (PLP) via the glutamine amidotransferase PLP synthase, a large enzyme complex of 12 Pdx1 synthase subunits with up to 12 Pdx2 glutaminase subunits attached. Deletion analysis revealed that the C-terminus has four distinct functionalities: assembly of the Pdx1 monomers, binding of the pentose substrate (ribose 5-phosphate), formation of the reaction intermediate I$_{320}$, and finally PLP synthesis. Deletions of distinct C-terminal regions distinguish between these individual functions. PLP formation is the only function that is conferred to the enzyme by the C-terminus acting *in trans*, explaining the cooperative nature of the complex.

Structured summary:
MINT-7994448: *PfPdx1* (uniprotkb:C6KT50) and *PfPdx1* (uniprotkb:C6KT50) bind (MI:0407) by *molecular sieving* (MI:0071)
MINT-7994425, MINT-7994413, MINT-7994435: *PfPdx1* (uniprotkb:C6KT50) and *PfPdx1* (uniprotkb:C6KT50) bind (MI:0407) by *cosedimentation in solution* (MI:0028).

1. Introduction

Malaria is caused by parasites of the genus *Plasmodium*. It is a disease that imposes a tremendous burden on global health putting over 2 billion people at risk and afflicting over 500 million people worldwide [1]. As current therapeutics are increasingly ineffective [2] and a clinically available vaccine is not in sight, there is an urgent need to identify and characterize new targets enabling novel chemotherapeutic strategies. The biosynthesis of vitamins is of particular interest in this respect, since the absence of these pathways in humans implies that their inhibition exclusively affects the metabolism of the parasite and not that of the human host. *Plasmodium* is able to synthesize certain vitamins *de novo*, either completely or in parts [3,4]. Among these is vitamin B$_6$ [5,6].

The term vitamin B$_6$ collectively refers to the vitamers pyridoxal, pyridoxine, pyridoxamine and their related phosphate esters. The metabolically active forms are pyridoxal 5-phosphate (PLP) und pyridoxamine 5-phosphate (PMP). PLP has been described as nature's most versatile cofactor and is involved in more than 100 enzymatic reactions [7,8]. In the malaria parasite, PLP is synthesized through the so-called deoxyxylose 5-phosphate independent pathway, in which the proteins Pdx1 and Pdx2 form a heteromeric class I glutamine amidotransferase [5,6]. The fully assembled PLP synthase complex consists of two interacting Pdx1 hexamers plus up to 12 Pdx2 molecules attached to them [9,23]. The glutaminase subunit Pdx2 generates ammonia – through the hydrolysis of glutamine – the source of the required ring nitrogen in the synthase reaction catalyzed by Pdx1 [11,12]. Ribose 5-phosphate (R5P) and glyceraldehyde 3-phosphate (G3P) are substrates of the synthase reaction catalysed by Pdx1 along with ammonia provided by Pdx2 [13].

The activity of the PLP synthase system is highly regulated [7,14–19]. Cooperativity between Pdx1 subunits is induced upon

binding of the pentose substrate [18]. Moreover, Pdx2 acts as an allosteric effector of Pdx1 when its substrate glutamine is bound and then further enhances the affinity of Pdx1 for R5P [18]. Combined cross-linking and mass spectrometry data suggest an inter-subunit cross-talk by interaction of the C-terminus of one subunit with a region immediately downstream of helix α8″ in the C-terminus of an adjoining monomer [18].

Here, we have investigated *Plasmodium falciparum* PLP synthase and report that helix α8″ is a prerequisite for hexamer assembly, and consequently for dodecamer formation. C-terminal deletion studies demonstrate that imine formation between R5P and K83 and subsequent conversion to the chromophoric I_{320} intermediate only requires six amino acid residues additional to helix α8″. However, full PLP synthetic activity then requires the native C-terminus. Hexamer/dodecamer formation is a prerequisite for covalent R5P-binding and accordingly for PLP synthase activity, however the glutaminase does not require an oligomeric Pdx1 complex for activation.

2. Materials and methods

2.1. Reagents

Antibiotics were purchased from AppliChem (Darmstadt, FRG), imidazole, 2-amino-2-(hydroxymethyl)-1,3-propanediol (Tris), NaCl, NH_4Cl, EDTA, Luria-Broth medium (LB), β-mercaptoethanol from Carl Roth (Karlsruhe, FRG), isopropyl β-D-1-thiogalactopyranoside (IPTG) was from PeqLab (Erlangen, FRG), L-glutamine, DL-G3P and R5P from Sigma–Aldrich (Taufkirchen, FRG). Restriction enzymes and DNA-polymerases were from New England Bioloabs (NEB, Schwalbach, FRG).

2.2. Molecular biology

Cloning of Pdx1 of *Plasmodium falciparum* (*Pf*Pdx1) into pET21a(+) has been described previously [5]. *Pf*Pdx1 and the C-terminally truncated versions *Pf*Pdx1$_{\Delta270–301}$, *Pf*Pdx1$_{\Delta273–301}$, *Pf*Pdx1$_{\Delta279–301}$ and *Pf*Pdx1$_{\Delta287–301}$ were generated by standard PCR and site mutagenesis using *Pf*Pdx1 as template and oligonucleotide primers as given in Supplement. All fragments were cloned via NdeI/XhoI restriction sites into pET28a(+) (Novagen, Merck, Nottingham, UK) generating N-terminally 6× His-tagged fusion proteins. The generation of additional deletion variants is described in Supplement.

2.3. Protein expression and purification

Plasmids were transformed into *E. coli* BL21-CodonPlus(DE3)-RIL cells (Stratagene, Amsterdam, NL) and expressed at 37 °C in LB medium containing 35 μg/ml chloramphenicol and 30 μg/ml kanamycin. The cells were induced at an OD_{600} of 0.5 with 0.1 mM IPTG. The bacteria were harvested after 3 h, washed with 150 mM NaCl and stored at −80 °C. For purification, the cell pellets were thawed and resuspended in lysis buffer (50 mM Tris–HCl pH 8.0, 300 mM NaCl, 20 mM imidazole, 10 mM β-mercaptoethanol) and disrupted by sonication. The lysate was cleared by centrifugation (30 min, 20 000×g, 4 °C) and applied to Ni-NTA agarose (QIAgen, Hilden, FRG). After washing with 40 mM imidazole the proteins were eluted with 200 mM imidazole in lysis buffer. Except for *Pf*Pdx1$_{\Delta279–301}$, the purified variants were concentrated using Amicon centrifugal filter devices with a molecular weight cut-off of 30 kDa (Millipore Corp., Billerica, USA) and applied to a Superdex 200 10/300 GL column (GE Healthcare, Freiburg, FRG) equilibrated with assay buffer (20 mM Tris–HCl pH 8.0, 10 mM NaCl, 0.5 mM EDTA). *Pf*Pdx1$_{\Delta279–301}$ interacted with the Superdex matrix, therefore fractions containing the variant were pooled after the Ni-NTA purification and dialysed over night against assay buffer.

2.4. Enzymatic assays

All variants were tested for PLP synthase activity as described in Refs. [5,19]. Formation of PLP was assayed using a Jasco V-550 spectrophotometer (Jasco, Groß-Umstadt, FRG) at a wavelength of 414 nm at 37 °C for 30 min. Formation of the I_{320} chromophoric intermediate was monitored at 315 nm [17]. 20 μM purified *Pf*Pdx1 or variants and 20 μM Pdx2 of *Plasmodium falciparum* (*Pf*Pdx2) were incubated in assay buffer in the presence of 1 mM R5P, 1 mM G3P and 10 mM L-glutamine. In the absence of *Pf*Pdx2, 10 mM NH_4Cl was used as nitrogen source. G3P was not added for the analysis of I_{320}-formation.

Glutaminase activity was determined as described previously [5]. Briefly, 5 μM of *Pf*Pdx1 or variants and 5 μM of *Pf*Pdx2 were incubated for 15 min at 30 °C with 10 mM L-glutamine, 0.5 mM 3-acetyl-pyridine adenine dinucleotide (APAD) and 10 U glutamate dehydrogenase. Reduction of APAD to APADH was monitored at 363 nm.

2.5. Static light scattering

To determine the absolute molecular weight without the use of internal standards, a gel filtration setup using a Superdex 200 10/300 GL size exclusion chromatography column (GE Healthcare, Freiburg, FRG) in line with static light scattering was used. The buffer used was 20 mM Tris–HCl pH 8.0, 100 mM NaCl. For in-line detection, a Mini Dawn light scattering instrument (Wyatt Technology, Dernbach, FRG) and a refractory index detector (WGE Dr. Bures, Dallgow, FRG) were used. Data were evaluated using the AstraV software (Wyatt Technology, Dernbach, FRG).

2.6. Analytical ultracentrifugation

The oligomeric states of *Pf*Pdx1 and all deletion variants were analysed by analytical ultracentrifugation (AUC). The sedimentation velocity was determined using a Beckman Optima XL-A ultracentrifuge (Beckman Coulter, USA). Runs were performed at 20 °C, 35 000 rpm or 42 000 rpm, λ = 280 nm, with a protein concentration of ∼65 μM in a buffer comprised of 20 mM Tris–HCl pH 8.0 and 100 mM NaCl. Buffer density, viscosities and protein partial specific volumes were calculated with the SEDNTERP program version 1.09 (http://www.rasmb.bbri.org, [20]). For analysis of the AUC data the program SEDFIT version 11.9b [21] was used. Calculations of sedimentation coefficients from the crystal structure coordinates were performed with the software HYDROPRO [22].

2.7. Mass spectrometry

Protein samples were purified using reversed phase μC4 micro-pipette tips (ZipTips, Millipore, Billerica, MA, USA) according to the manufacturers' protocol. NanoESI-MS experiments were carried out on a QTOF2 mass spectrometer (Waters, Micromass, Manchester, UK). Samples were sprayed from in-house produced gold coated spray needles. Static electrospray was established by applying a capillary voltage of 1000 V. Data acquired were analyzed by MassLynx 4.1.

3. Results

The C-terminal region of Pdx1 is responsible for intersubunit cross-talk and confers cooperativity to the enzyme [18]. The full C-terminus of Pdx1 is not resolved in prokaryotic 3D structures [9,10,23] and in these structures helix α8″ is the most C-terminal secondary structure element in the core of Pdx1 (Fig. 1A). However, a substantial portion of the C-terminus has been resolved with the
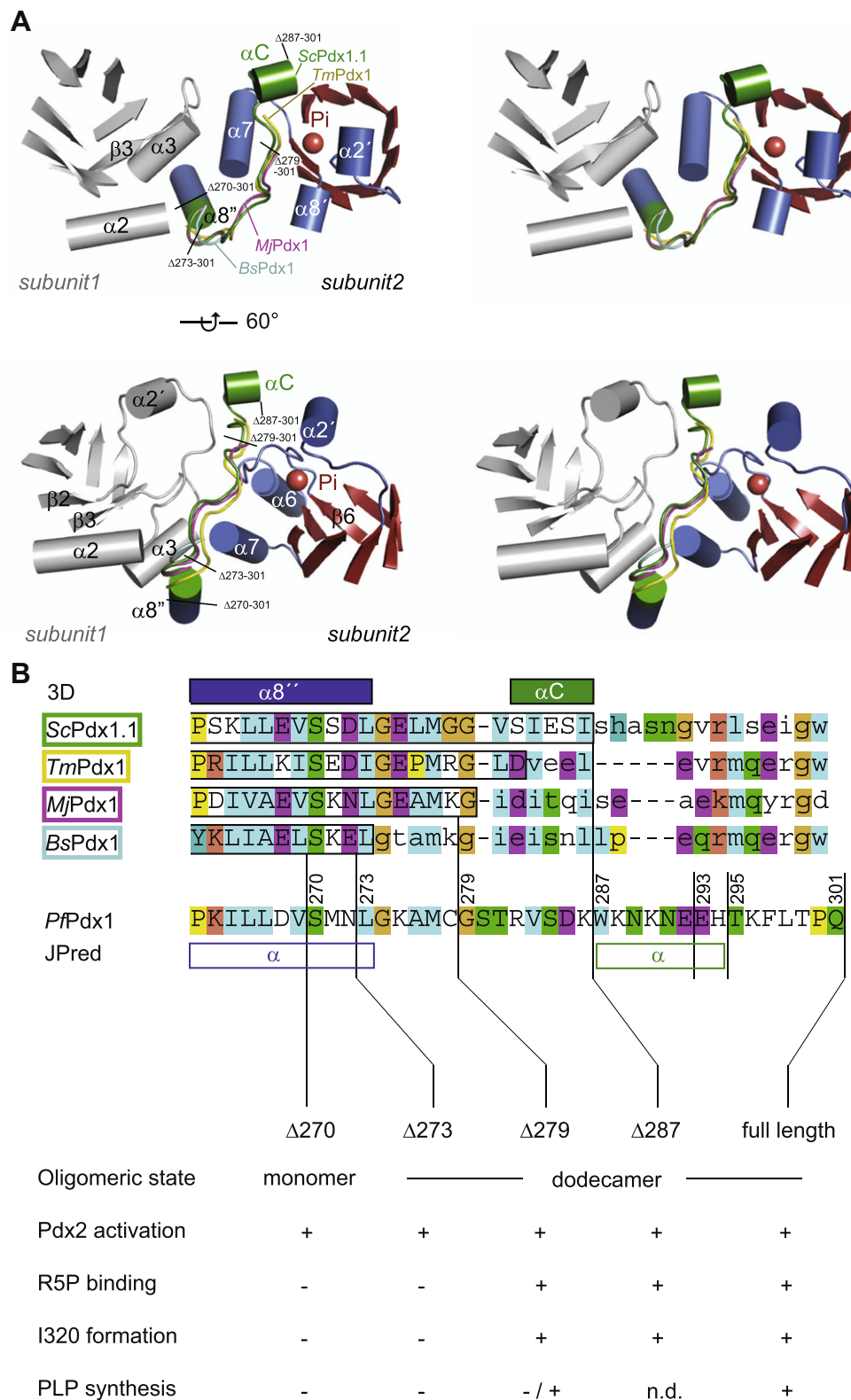
Fig. 1. Deletion analysis of Pdx1 of *Plasmodium falciparam*. (A) Shown is the structure of *Saccharomyces cerevisiae* Pdx1 (3FEM); two stereo views of adjacent subunits of one hexamer are presented. Large parts of the 3D structure have been omitted for clarity. The C-terminal regions of previously determined structures from Thermotoga maritima (TmPdx1, yellow, 2ISS), *Methanocaldococcus jannaschii* (MjPdx1, magenta, 2YZR) and *Bacillus subtilis* (BsPdx1, blue, 2NV2) are also shown. Pi stands for inorganic phosphate and indicates the binding site for the substrate pentose phosphate. (B) The alignment displays the relevant sequences and the secondary structure assignment. In the alignment, amino acids present in the 3D structure are given in capital and boxed. The sequence of PfPdx1 is given with a secondary structure prediction using Jpred 3 [26]. The table lists enzymatic activities and oligomeric state for the referenced PfPdx1 deletion variants. n.d.: not determined.

3D structure of the eukaryotic Pdx1 protein from *Saccharomyces cerevisiae* [24]. In the yeast structure, helix α8″ is followed by a

random coil region leading into helix αC [24]. Remarkably, the partly resolved random coil regions of the bacterial structures

Table 1
Biochemical characterization of PfPdx1 and its C-terminal truncation variants using NH$_4$Cl as ammonium donor.

Protein	R5P-binding[a]	I$_{320}$-specific activity		PLP-specific activity		Oligomeric state[b]
		nmol min^{-1} mg^{-1}	%	pmol min^{-1} mg^{-1}	%	
PfPdx1	+	1.22 ± 0.04	100	695 ± 71	100	Dodecamer
PfPdx1$_{\Delta270-301}$	−	n.d.	0	n.d.	0	Mainly monomer
PfPdx1$_{\Delta273-301}$	−	n.d.	0	n.d.	0	Dodecamer
PfPdx1$_{\Delta279-301}$	+	1.3 ± 0.4	107	351 ± 77	51	Dodecamer
PfPdx1$_{\Delta287-301}$	+	1.9 ± 0.2	155	−[c]	−[c]	Dodecamer

Assays were performed with 20 μM protein, 1 mM R5P, 1 mM G3P, 10 mM NH$_4$Cl in 20 mM Tris–HCl pH 8.0, 10 mM NaCl, 0.5 mM EDTA. The activity of PfPdx1 was set as 100 %. Experimental results are means of at least three independent measurements. n.d.: none detected.

[a] Compare Table 4.
[b] Compare Table 3.
[c] Protein precipitated upon addition of G3P.

and the yeast structure superpose well, suggesting relevance of the observed conformation in this region (Fig. 1A).

Secondary structure predictions for the C-terminus of PfPdx1 confirm the positioning of helix α8″, however, the predicted C-terminal helix αC is shifted and extended compared to that of Saccharomyces Pdx1. Based on this analysis, we designed the following C-terminal deletion variants: PfPdx1$_{\Delta270-301}$, truncating the protein at the last turn of helix α8″; PfPdx1$_{\Delta273-301}$, truncating the protein immediately after helix α8″; PfPdx1$_{\Delta279-301}$, truncating the protein between helices α8″ and αC; and finally PfPdx1$_{\Delta287-301}$, truncating the protein after the resolved part of helix αC in S. cerevisiae Pdx1 but before the predicted helix αC of P. falciparum (Fig. 1B; additional variants indicated in the figure are presented in Supplement). After expression and purification, the variants were characterized with respect to their oligomeric state and their abilities to bind R5P, to form the chromophoric reaction intermediate I$_{320}$ [13,17] and to synthesise PLP [5]. Furthermore, the glutaminase activity of the Pdx1/Pdx2 complex was determined [5].

The oligomerisation behaviour of Pdx1 was altered in the shortest variant, PfPdx1$_{\Delta270-301}$, as determined by analytical ultracentrifugation (Tables 1 and 3, Fig. 2A). This behaviour was independently confirmed by size exclusion chromatography coupled with static light scattering (Fig. 2B). The dominant species was the monomer with a sedimentation coefficient of 3.0 ± 0.1 S making up roughly two thirds (68%) of the total protein. Species with sedimentation coefficients of 4.8 ± 0.5 S and 6.9 ± 1.1 S corresponding roughly to dimeric and tetrameric forms were also present. The

analytical ultracentrifugation data displayed broad peaks for the oligomeric species suggesting a fast equilibrium between several states (Fig. 2A). Interestingly, PfPdx1$_{\Delta270-301}$ was able to fully activate the glutaminase Pdx2, suggesting that the monomeric species retained this propensity (Table 2). This also suggests that this truncation variant possesses an intact Pdx1–Pdx2 interface.

PfPdx1$_{\Delta270-301}$ proved to be catalytically inactive for I$_{320}$ and PLP formation either alone or in complex with PfPdx2 (Tables 1 and 2). This prompted us to investigate whether this variant is able to bind R5P. PfPdx1$_{\Delta270-301}$ was incubated with R5P and the molecular mass was determined by ESI-MS. When wild-type PfPdx1 is incubated with R5P, the determined molecular mass in ESI-MS changes by 212 Da, reflecting the formation of a covalent Schiff base between R5P and the catalytic lysine 83 (Table 4) [10,14,17,18]. However, the molecular mass of PfPdx1$_{\Delta270-301}$ remained unaltered upon incubation with R5P, indicating that this variant is incapable of forming the covalent imine intermediate with its pentose substrate (Tables 1 and 4).

In PfPdx1$_{\Delta270-301}$, PfPdx1 is truncated within helix α8″ which is at the oligomerisation interface. Hence the deletion mutant PfPdx1$_{\Delta273-301}$ was examined in which the truncation occurs just after helix α8″ and this protein was found to form dodecamers (Tables 1 and 3). The three additional amino acids in PfPdx1$_{\Delta273-301}$ are a conserved serine that makes a hydrophilic contact with a backbone atom of the preceding helical turn followed by two solvent exposed and variable residues. A mutant in which the serine was replaced by an alanine (PfPdx1$_{S270A\Delta273-301}$ variant; see
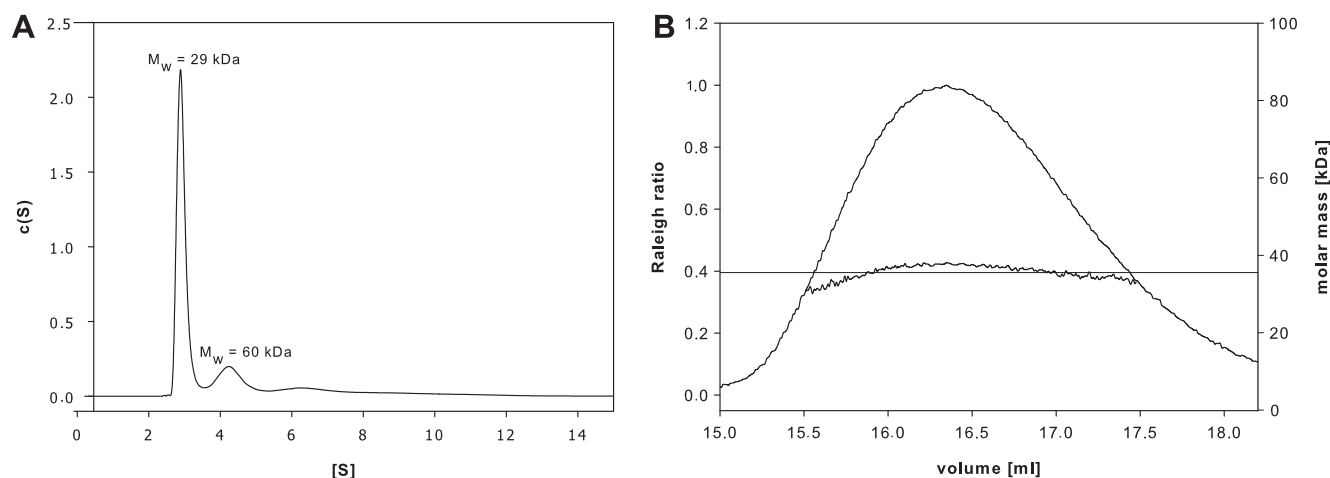
Fig. 2. Oligomeric nature of PfPdx1$_{\Delta270-301}$ analyzed in solution (A) the main peak observed in sedimentation velocity analytical ultracentrifugation is fitted to a sedimentation coefficient s = 3.0 S, which corresponds to a monomeric species with a molecular mass of 29 kDa. The sedimentation coefficients of the minor peaks were at 4.8 S and 6.9 S, respectively. These represent higher oligomeric forms that appear to be in a rapid equilibrium, as suggested by the shallow shape of the peaks. (B) For absolute mass determination without use of internal standards, size exclusion chromatography in line with RI-detection and static light scattering was performed. The fitted molecular mass of the observed peak was 35 kDa ± 2%.

Table 2
Biochemical characterization of PfPdx1 and its C-terminal truncation variants in presence of PfPdx2.

Protein + PfPdx2	I$_{320}$-specific activity		PLP-specific activity		Glutaminase-specific activity	
	nmol min^{-1} mg^{-1}	%	pmol min^{-1} mg^{-1}	%	nmol min^{-1} mg^{-1}	%
PfPdx1	2.76 ± 0.2	100	779 ± 130	100	193.90 ± 14	100
PfPdx1$_{\Delta270–301}$	n.d	0	n.d.	0	190.60 ± 3	99
PfPdx1$_{\Delta273–301}$	n.d	0	n.d.	0	202.77 ± 16	105
PfPdx1$_{\Delta279–301}$	4.62 ± 0.4	167	250 ± 32	32	271.62 ± 8	140
PfPdx1$_{\Delta287–301}$	2.25 ± 0.1	83	–[a]	–[a]	182.76 ± 9	94

Assays were performed with 20 μM protein, 1 mM R5P, 1 mM G3P, 10 mM L-glutamine in 20 mM Tris–HCl pH 8.0, 10 mM NaCl, 0.5 mM EDTA. The activity of PfPdx1/PfPdx2 was set as 100%. Experimental results are means of at least three independent measurements. n.d. – none detected.
[a] – Protein precipitated on addition of G3P.

Table 3
Analysis of Pdx1 and the C-terminal truncation variants by analytical ultracentrifugation (velocity sedimentation).

Protein	s_{exp} (S)[a]	M_{exp} (kDa)[b]	M_{cal} (kDa)[c]
PfPdx1	14.0	363	420
PfPdx1$_{\Delta270–301}$[d]	Peak 1: 3.0 ± 0.1	29 ± 3	31
	Peak 2: 4.8 ± 0.5	60 ± 12	–
	Peak 3: 6.9 ± 1.1	110 ± 26	–
PfPdx1$_{\Delta273–301}$	12.9	324	380
PfPdx1$_{\Delta279–301}$	13.0	330	387
PfPdx1$_{\Delta287–301}$	13.8	354	400

[a] The $c(S)$ distribution of sedimentation coefficients was determined with SEDFIT [21] and corrected to standard conditions (20 °C, H$_2$O). Calculated s values using HYDROPRO and 3.1 Å bead size [22] are 2.7 S for the monomeric and 15.4 S for the dodecameric species.
[b] Molecular mass derived from molar mass distributions $c(M)$ calculated by SEDFIT. For all dodecameric variants the frictional ratio was fixed to 1.25 (average of all experiments).
[c] Molecular mass calculated from the amino acid composition.
[d] Three different species were detected. The monomeric form fitted to 3.0 ± 0.1 S and comprised about two thirds of the total protein. The standard deviation is given on the basis of three independent experiments. Higher oligomeric forms are probably in fast equilibrium giving rise to larger errors as discussed in the text (no theoretical s and M values calculated).

Table 4
Molecular mass of PfPdx1 and the C-terminal truncation variants in the absence or presence of ribose 5-phosphate as determined by ESI-MS.

Protein	−R5P (Da)	+R5P (Da)
PfPdx1	35320.7	35532.6
PfPdx1$_{\Delta270–301}$	31506.8	31506.8
PfPdx1$_{\Delta273–301}$	31722.6	31722.6

Supplement Tables S1 and S3) was dodecameric, suggesting that the length of the helical segment is crucial for the integrity of the oligomerisation interface.

The PfPdx1$_{\Delta273–301}$ variant was unable to produce the chromophoric reaction intermediate I$_{320}$ and, consequently, has no PLP synthetic activity (Tables 1 and 2). Similarly, the BsPdx1$_{\Delta273–294}$ variant, roughly equivalent to PfPdx1$_{\Delta273–301}$ but containing two additional amino acids at the C-terminus, was severely impaired in the formation of the chromophore (0.5% of wild-type activity) and displayed no detectable PLP synthase activity [18]. Using ESI-MS, we could show that PfPdx1$_{\Delta273–301}$ was unable to covalently bind the pentose substrate (Tables 1 and 4). However, PfPdx1$_{\Delta273–301}$ was able to fully activate PfPdx2 similarly to the wild-type protein (Table 2).

Inclusion of additional six amino acid residues in PfPdx1$_{\Delta279–301}$ elicits chromophore-specific activity. This variant is dodecameric in nature (Tables 1 and 3) and shows chromophore-specific activity similar to the wild-type protein, whereas PLP-specific activity was halved (Table 1). The six additional amino acids, of which glycine

274 and methionine 277 are conserved among Pdx1 orthologs, are thus required for imine formation with R5P and the formation of the chromophoric intermediate. I$_{320}$-specific activity increased above that of wild-type in the Pdx2-dependent assay (167% versus 100%; Table 2), while PLP-specific activity was further reduced (32%; Table 2). Thus, Pdx2 in its glutamine bound form has an influence on chromophore formation, exerting an allosteric effect [18], even when only the truncated form is considered.

PfPdx1$_{\Delta287–301}$ contains the segment equivalent to the resolved part of helix αC of the S. cerivisiae Pdx1. This variant forms dodecamers and exhibits chromophore-specific activity (Tables 1–3). Unlike PfPdx1$_{\Delta279–301}$, the I$_{320}$-specific activity of PfPdx1$_{\Delta287–301}$ was greater than that of wild-type in the absence of Pdx2 (155% versus 100%), but slightly decreased in the presence of Pdx2 (83% versus 100%) (Tables 1 and 2). Further, no PLP-specific activity could be determined for PfPdx1$_{\Delta287–301}$, since addition of G3P resulted in an instantaneous precipitation of the protein. Indeed, we have tested two further deletion variants and observed the same behaviour and similar stability problems (PfPdx1$_{\Delta293–301}$ and PfPdx1$_{\Delta295–301}$, see Supplement). The very C-terminus with the predicted C-terminal helix likely is an independent functional domain allowing Pdx1 to accommodate conformational changes that occur upon or as a consequence of G3P binding. If the integrity of this domain is disturbed, G3P integration into the forming PLP molecule is impaired. Thus, only the native C-terminus ensures optimal PLP biosynthesis.

4. Discussion

The C-terminus of Pdx1, which has evaded structural determination, is essential for catalytic activity of the protein [18]. In the current study, we performed a deletion analysis and assigned specific functions to defined regions of the C-terminus. Variants were characterized with respect to (i) their ability to form the hexamer/dodecamer state of wild-type protein, (ii) their enzymatic properties, i.e., substrate binding, I$_{320}$-formation and PLP synthesis, and (iii) their ability to activate Pdx2, the glutaminase partner.

The PfPdx1$_{\Delta270–301}$ variant with truncated helix α8″ was the only variant that had defective oligomerization behaviour. This protein adopted several oligomeric states with the monomer being the predominant species (Fig. 2). The other deletion variants tested here showed dodecameric organization. Thus, integrity of helix α8″ is essential to stabilize the oligomer, as can be proposed on the basis of crystallographic analyses [9,10,23]. Exchanges of conserved amino acid residues in the loop preceding helix α3, which likewise are at the interface between protamers, also affected the oligomerisation behaviour of Pdx1 [25].

Interestingly, the PfPdx1$_{\Delta270–301}$ variant was able to fully activate the glutaminase PfPdx2 (Table 2). It is possible that this activity is due to presence of transient hexamers. However, glutaminase activation is identical to native PfPdx1/PfPdx2 complexes and on

this basis we propose that a Pdx1 monomer is able to interact with and activate the Pdx2 glutaminase. Importantly, this is in contrast to the earlier finding that the monomeric Pdx1 variant with exchanges of conserved amino acid residues in the loop preceding helix α3 was unable to activate the glutaminase partner Pdx2 [25].

Neither $PfPdx1_{\Delta270-301}$ nor $PfPdx1_{\Delta273-301}$ was capable of covalently binding the substrate R5P. This suggests that a Pdx1 dodecamer is required for binding of the pentose substrate and that the protein must extend over the "minimal" core as represented by the $PfPdx1_{\Delta273-301}$ variant. The $PfPdx1_{\Delta279-301}$ variant then binds R5P and also forms the I_{320} intermediate and PLP. Full PLP synthase activity, however, requires the native C-terminus from amino acid 279 onward. Thus, within the C-terminal segment investigated here, R5P-binding and I_{320}-formation are assigned to amino acids 273–278.

The C-terminal region from residue 273 on is in close proximity to helix α8′ and the loop between β6 and α6 of the $(\beta\alpha)_8$-barrel (Fig. 1A) both of which have been implied in phosphate binding of the substrate R5P [10]. It is likely that the C-terminal segment helps organising the whole structural region and in consequence substrate binding, because of two reasons: the observed close proximity and the observation that the C-terminal segment superposes well in all structures, where it was resolved (Fig. 1A).

The $PfPdx1_{\Delta279-301}$ variant is competent for PLP formation, however, at a reduced level (Tables 1 and 2). It is therefore quite likely that the C-terminus beyond Cys278 including helix αC is an independent domain required for optimal PLP production. Interestingly, helix αC is in close proximity to helix α2′ of a neighbouring subunit [24]. This likely explains the observed cooperativity in the oligomeric enzyme [18]. Raschle et al. proposed that the C-terminus may act as a lid to close the active site, and they proposed this function is dependent on presence of R5P [18]. The structural and mutational analysis presented here now suggests that the first part of the C-terminus acts in cis, organising phosphate binding of the pentose substrate, while, by analogy to the S. cerevisiae structure, the very C-terminus from helix αC onward acts in trans, organising the α2′ region, likewise implied in pentose binding. The truncation variant $PfPdx1_{\Delta279-301}$ cannot interact with a neighbouring subunit in the proposed way and consequently lacks full PLP synthase activity. In contrast, the $PfPdx1_{\Delta287-301}$ variant would be able to interact in trans with the α2′ region, but because it precipitated upon addition of G3P – as do the variants, which were truncated C-terminally of $PfPdx1_{\Delta287-301}$ – formation of PLP could not be determined making it impossible to further analyze this region. We conclude that the region C-terminal to helix αC further enhances PLP formation, presumably by mediating G3P binding and/or steps subsequent to G3P incorporation. Together, the data argue for an important structural role of the C-terminus in catalysis, which explains the rather limited conservation in this region and probably the lack of consensus catalytic residues.

Acknowledgement

Appendix A. Supplementary data

Supplementary data associated with this article can be found, in the online version, at doi:10.1016/j.febslet.2010.09.013.

References

[1] Snow, R.W., Guerra, C.A., Noor, A.M., Myint, H.Y. and Hay, S.I. (2005) The global distribution of clinical episodes of Plasmodium falciparum malaria. Nature 434, 214–217.

[2] Guerin, P.J., Bates, S.J. and Sibley, C.H. (2009) Global resistance surveillance: ensuring antimalarial efficacy in the future. Curr. Opin. Infect. Dis. 22, 593–600.

[3] Muller, I.B., Hyde, J.E. and Wrenger, C. (2009) Vitamin B metabolism in Plasmodium falciparum as a source of drug targets. Trends Parasitol. 26, 35–43.

[4] Muller, S. and Kappes, B. (2007) Vitamin and cofactor biosynthesis pathways in Plasmodium and other apicomplexan parasites. Trends Parasitol. 23, 112–121.

[5] Gengenbacher, M. et al. (2006) Vitamin B6 biosynthesis by the malaria parasite Plasmodium falciparum: biochemical and structural insights. J. Biol. Chem. 281, 3633–3641.

[6] Wrenger, C., Eschbach, M.L., Muller, I.B., Warnecke, D. and Walter, R.D. (2005) Analysis of the vitamin B6 biosynthesis pathway in the human malaria parasite Plasmodium falciparum. J. Biol. Chem. 280, 5242–5248.

[7] Fitzpatrick, T.B., Amrhein, N., Kappes, B., Macheroux, P., Tews, I. and Raschle, T. (2007) Two independent routes of de novo vitamin B6 biosynthesis: not that different after all. Biochem. J. 407, 1–13.

[8] Mozzarelli, A. and Bettati, S. (2006) Exploring the pyridoxal 5'-phosphate-dependent enzymes. Chem. Rec. 6, 275–287.

[9] Strohmeier, M., Raschle, T., Mazurkiewicz, J., Rippe, K., Sinning, I., Fitzpatrick, T.B. and Tews, I. (2006) Structure of a bacterial pyridoxal 5'-phosphate synthase complex. Proc. Natl. Acad. Sci. USA 103, 19284–19289.

[10] Zein, F., Zhang, Y., Kang, Y.N., Burns, K., Begley, T.P. and Ealick, S.E. (2006) Structural insights into the mechanism of the PLP synthase holoenzyme from Thermotoga maritima. Biochemistry 45, 14609–14620.

[11] Tazuya, K., Adachi, Y., Masuda, K., Yamada, K. and Kumaoka, H. (1995) Origin of the nitrogen atom of pyridoxine in Saccharomyces cerevisiae. Biochim. Biophys. Acta 1244, 113–116.

[12] Zalkin, H. and Smith, J.L. (1998) Enzymes utilizing glutamine as an amide donor. Adv. Enzymol. Relat. Areas Mol. Biol. 72, 87–144.

[13] Hanes, J.W., Keresztes, I. and Begley, T.P. (2008) ^{13}C NMR snapshots of the complex reaction coordinate of pyridoxal phosphate synthase. Nat. Chem. Biol. 4, 425–430.

[14] Burns, K.E., Xiang, Y., Kinsland, C.L., McLafferty, F.W. and Begley, T.P. (2005) Reconstitution and biochemical characterization of a new pyridoxal-5'-phosphate biosynthetic pathway. J. Am. Chem. Soc. 127, 3682–3683.

[15] Flicker, K., Neuwirth, M., Strohmeier, M., Kappes, B., Tews, I. and Macheroux, P. (2007) Structural and thermodynamic insights into the assembly of the heteromeric pyridoxal phosphate synthase from Plasmodium falciparum. J. Mol. Biol. 374, 732–748.

[16] Neuwirth, M., Flicker, K., Strohmeier, M., Tews, I. and Macheroux, P. (2007) Thermodynamic characterization of the protein–protein interaction in the heteromeric Bacillus subtilis pyridoxal phosphate synthase. Biochemistry 46, 5131–5139.

[17] Raschle, T., Arigoni, D., Brunisholz, R., Rechsteiner, H., Amrhein, N. and Fitzpatrick, T.B. (2007) Reaction mechanism of pyridoxal 5'-phosphate synthase. Detection of an enzyme-bound chromophoric intermediate. J. Biol. Chem. 282, 6098–6105.

[18] Raschle, T., Speziga, D., Kress, W., Moccand, C., Gehrig, P., Amrhein, N., Weber-Ban, E. and Fitzpatrick, T.B. (2009) Intersubunit cross-talk in pyridoxal 5'-phosphate synthase, coordinated by the C terminus of the synthase subunit. J. Biol. Chem. 284, 7706–7718.

[19] Raschle, T., Amrhein, N. and Fitzpatrick, T.B. (2005) On the two components of pyridoxal 5'-phosphate synthase from Bacillus subtilis. J. Biol. Chem. 280, 32291–32300.

[20] Laue, T.M., Shah, B.D., Ridgeway, T.M. and Pelletier, S.L. (1992) Computer-Aided Interpretation of Analytical Sedimentation Data for Proteins in: Analytical Ultracentrifugation in Biochemistry and Polymer Science (Harding, S.E., Rowe, A.J. and Horton, J.C., Eds.), pp. 90–125, The Royal Society of Chemistry, Cambridge, UK.

[21] Dam, J. and Schuck, P. (2004) Calculating sedimentation coefficient distributions by direct modeling of sedimentation velocity concentration profiles. Methods Enzymol. 384, 185–212.

[22] Garcia De La Torre, J., Huertas, M.L. and Carrasco, B. (2000) Calculation of hydrodynamic properties of globular proteins from their atomic-level structure. Biophys. J. 78, 719–730.

[23] Zhu, J., Burgner, J.W., Harms, E., Belitsky, B.R. and Smith, J.L. (2005) A new arrangement of (beta/alpha)8 barrels in the synthase subunit of PLP synthase. J. Biol. Chem. 280, 27914–27923.

[24] Neuwirth, M. et al. (2009) X-ray crystal structure of Saccharomyces cerevisiae Pdx1 provides insights into the oligomeric nature of PLP synthases. FEBS Lett. 583, 2179–2186.

[25] Muller, I.B., Knockel, J., Groves, M.R., Jordanova, R., Ealick, S.E., Walter, R.D. and Wrenger, C. (2008) The assembly of the plasmodial PLP synthase complex follows a defined course. PLoS One 3, e1815.

[26] Cole, C., Barber, J.D. and Barton, G.J. (2008) The Jpred 3 secondary structure prediction server. Nucleic Acids Res. 36, W197–W201.

Supplement

Oligonucleotides used for the generation of the variants Pf*Pdx1,* Pf*Pdx1$_{\Delta270\text{-}301}$,* Pf*Pdx1$_{\Delta273\text{-}301}$,* Pf*Pdx1$_{\Delta279\text{-}301}$ and* Pf*Pdx1$_{\Delta287\text{-}301}$*

For the generation of *Pf*Pdx1, *Pf*Pdx1$_{\Delta270\text{-}301}$, *Pf*Pdx1$_{\Delta273\text{-}301}$, *Pf*Pdx1$_{\Delta279\text{-}301}$ and *Pf*Pdx1$_{\Delta287\text{-}301}$ the following primer pairs were used: *Pf*Pdx1 (*Pf*Pdx1.fwd (5'-GAAGAAGGATCCATATGGAAAATCATAAAGATGATGCAG-3'/ PfPdx1_stop_XhoI.rev (5'-CGGCGGCTCGAGTTATTGTGGTGTTAAAAATTTGGTGTGTTCTTC-3')), *Pf*Pdx1$_{\Delta270\text{-}301}$ (*Pf*Pdx1$_{\Delta270\text{-}301}$.fwd (5'-CTAAAATACTTTTAGATGTTTGATAGCTCGAG-3')/ *Pf*Pdx1$_{\Delta270\text{-}301}$.rev (5'-TTTCTCGAGCTATCAAACATCTAAAGTATTTTAG-3')), *Pf*Pdx1$_{\Delta273\text{-}301}$ (*Pf*Pdx1.fwd (5'-GAAGAAGGATCCATATGGAAAATCATAAAGATGATGCAG-3'/ *Pf*Pdx1$_{\Delta273\text{-}301}$.rev (5'-TAATAACTCGAGTTAATTCATACTAACATCTAAAGTATTTTAGG-3')), *Pf*Pdx1$_{\Delta279\text{-}301}$ (*Pf*Pdx1$_{\Delta279\text{-}301}$.fwd (5'-GGAAAAGCCATGTGTTGATAGCTCGAGAAAA-3')/ *Pf*Pdx1$_{\Delta279\text{-}301}$.rev (5'-TTTTCTCGAGCTATCACACATGGCTTTTCC-3')) and *Pf*Pdx1$_{\Delta287\text{-}301}$ (*Pf*Pdx1.fwd (5'-GAAGAAGGATCCATATGGAAAATCATAAAGATGATGCAG-3'/ *Pf*Pdx1$_{\Delta287\text{-}301}$.rev (5'-TAATAACTCGAGTTATTTATCCGAACGCGTGTGC-3')).

Generation of the variants Pf*Pdx1$_{\Delta293\text{-}301}$,* Pf*Pdx1$_{\Delta295\text{-}301}$ and* Pf*Pdx1$_{S270A\Delta273\text{-}301}$*

The variants *Pf*Pdx1$_{\Delta293\text{-}301}$, *Pf*Pdx1$_{\Delta295\text{-}301}$ and *Pf*Pdx1$_{S270A\Delta273\text{-}301}$ have been generated in the same way as the variants described in the main publication using the following primers pairs: *Pf*Pdx1$_{\Delta293\text{-}301}$ (*Pf*Pdx1$_{\Delta293\text{-}301}$.fwd (5'-AAAAACTCGAGCTATTATTCATTTTTATTTTTCC-3')/ *Pf*Pdx1$_{\Delta293\text{-}301}$.rev (5'-GGAAAAATAAAAATGAATAATAGCTCGAGTTTTT-3')), *Pf*Pdx1$_{\Delta295\text{-}301}$ (*Pf*Pdx1.fwd

Derrer et al.

(5'-GAAGAAGGATCCATATGGAAAATCATAAAGATGATGCAG-3'/ *Pf*Pdx1$_{\Delta295-301}$.rev

(5'-TAATAACTCGAGTTAGTGTTCTTCATTTTTATTTTTCCATTTATCC-3'),

*Pf*Pdx1$_{S270A\Delta273-301}$

(*Pf*Pdx1.fwd (5'-GAAGAAGGATCCATATGGAAAATCATAAAGATGATGCAG-3'/

*Pf*Pdx1$_{S270A\Delta273-301}$.rev (5'-

TAATAACTCGAGTTAATTCATTGCAACATCTAAAGTATTTTAGGGTTATTAAAAT

TGC-3').

Derrer et al.

Table S1

protein	R5P binding[a]	I$_{320}$-specific activity		PLP-specific activity		Oligomeric state[b]
		nmol min^{-1} mg^{-1}	%	pmol min^{-1} mg^{-1}	%	
*Pf*Pdx1	+	1.22 ± 0.04	100	695 ± 71	100	dodecamer
*Pf*Pdx1$_{\Delta270\text{-}301}$	-	n.d.	0	n.d.	0	mainly monomer
*Pf*Pdx1$_{\Delta273\text{-}301}$	-	n.d.	0	n.d.	0	dodecamer
*Pf*Pdx1$_{\Delta279\text{-}301}$	+	1.3 ± 0.4	107	351 ± 77	51	dodecamer
*Pf*Pdx1$_{\Delta287\text{-}301}$	+	1.9 ± 0.2	155	-[c]	-[c]	dodecamer
*Pf*Pdx1$_{\Delta295\text{-}301}$	+	1.75 ± 0.1	143	-	-	dodecamer
*Pf*Pdx1$_{S270A\Delta273\text{-}301}$	-	n.d	0	n.d	0	dodecamer

Biochemical characterization of *Pf*Pdx1 and its C-terminal truncation variants using NH$_4$Cl as ammonium donor. Assays were performed with 20 µM protein, 1 mM R5P, 1 mM G3P, 10 mM NH$_4$Cl in 20 mM Tris-HCl pH 8.0, 10 mM NaCl, 0.5 mM EDTA. The activity of *Pf*Pdx1 was set as 100 %. Experimental results are means of at least three different measurements. n.d.: not detected; [a] compare Table 4; [b] compare Table 3; [c] protein precipitated upon addition of G3P.

Derrer et al.

Table S2

Protein + PfPdx2	I_{320}-specific activity		PLP-specific activity		Glutaminase-specific activity	
	nmol min^{-1} mg^{-1}	%	pmol min^{-1} mg^{-1}	%	nmol min^{-1} mg^{-1}	%
PfPdx1	2.76 ± 0.2	100	779 ± 130	100	193.9 ± 14	100
PfPdx1$_{\Delta270\text{-}301}$	n.d	0	n.d.	0	190.60 ± 3	99
PfPdx1$_{\Delta273\text{-}301}$	n.d	0	n.d.	0	202.77 ± 16	105
PfPdx1$_{\Delta279\text{-}301}$	4.62 ± 0.4	167	250 ± 32	32	271.62 ± 8	140
PfPdx1$_{\Delta287\text{-}301}$	2.25 ± 0.1	83	-[a]	-[a]	182.76 ± 9	94
PfPdx1$_{\Delta295\text{-}301}$	1.75 ± 0.1	63	-[a]	-[a]	200.75 ± 11	103
PfPdx1$_{S270A\Delta273\text{-}301}$	n.d.	0	n.d	0	160.8 ± 4	87

Biochemical characterization of PfPdx1 and its C-terminal truncation variants in presence of PfPdx2. Assays were performed with 20 μM protein, 1 mM R5P, 1 mM G3P, 10 mM L-glutamine in 20 mM Tris-HCl pH 8.0, 10 mM NaCl, 0.5 mM EDTA. The activity of PfPdx1/PfPdx2 was set as 100 %. Experimental results are means of at least three different measurements. n.d. - none detected. [a] - protein precipitated on addition of G3P.

Derrer et al.

Table S3

Analysis of Pdx1 and the C-terminal truncation variants by analytical ultracentrifugation (velocity sedimentation)

Protein	s_{exp} (S)[a]	M_{exp} (kDa)[b]	M_{cal} (kDa)[c]
*Pf*Pdx1	14.0	363	420
*Pf*Pdx1$_{\Delta270-301}$[d]	Peak 1: 3.0 ± 0.1 Peak 2: 4.8 ± 0.5 Peak 3: 6.9 ± 1.1	29 ± 3 60 ± 12 110 ± 26	31 - -
*Pf*Pdx1$_{\Delta273-301}$	12.9	324	380
*Pf*Pdx1$_{\Delta279-301}$	13.0	330	387
*Pf*Pdx1$_{\Delta287-301}$	13.8	354	400
*Pf*Pdx1$_{\Delta295-301}$	13.6	340	412
*Pf*Pdx1$_{S270A\Delta273-301}$	13.0	319	382

[a] The c(S) distribution of sedimentation coefficients was determined with SEDFIT [21] and corrected to standard conditions (20 °C, H_2O). Calculated *s*-values using HYDROPRO and 3.1-Å bead size [22] are 2.7 S for the monomeric and 15.4 S for the dodecameric species.
[b] Molecular mass derived from molar mass distributions c(M) calculated by SEDFIT. For all dodecameric variants the frictional ratio was fixed to 1.25 (average of all experiments).
[c] Molecular mass calculated from the amino acid composition.
[d] Three different species were detected. The monomeric form fitted to 3.0 ± 0.1 S and comprised about two thirds of the total protein. The standard deviation is given on the basis of three independent experiments. Higher oligomeric forms are probably in fast equilibrium giving rise to larger errors as discussed in the text (no theoretical *s* and *M* values calculated).

Derrer et al.

Table 4

Molecular mass of *Pf*Pdx1 and the C-terminal truncation variants in the absence or presence
of ribose 5-phosphate as determined by ESI-MS

Protein	- R5P (Da)	+ R5P (Da)
*Pf*Pdx1	35,320.7	35,532.6
*Pf*Pdx1$_{\Delta270\text{-}301}$	31,506.8	31,506.8
*Pf*Pdx1$_{\Delta273\text{-}301}$	31,722.6	31,722.6